Catalysts **2014**, *4*, 414-426; doi:10.3390/catal4040414

OPEN ACCESS

catalysts

ISSN 2073-4344

www.mdpi.com/journal/catalysts

Article

Valorisation of Vietnamese Rice Straw Waste: Catalytic Aqueous Phase Reforming of Hydrolysate from Steam Explosion to Platform Chemicals

Cao Huong Giang [1], Amin Osatiashtiani [2], Vannia Cristina dos Santos [3], Adam F. Lee [2,*], David R. Wilson [4], Keith W. Waldron [4] and Karen Wilson [2,*]

[1] Vietnam Academy of Agricultural Science, Vinh Quynh, Thanh Tri, Ha Noi, Vietnam; E-Mail: caohuonggiang84vn@gmail.com

[2] European Bioenergy Research Institute, School of Engineering and Applied Sciences, Aston University, Birmingham B4 7ET, UK; E-Mail: a.osatiashtiani@aston.ac.uk

[3] Laboratory of Bioinorganic Chemistry and Catalysis, Federal University of Paraná, CP 19081, CEP 81531-990, Curitiba, Paraná, Brazil; E-Mail: vanniasantos@yahoo.com.br

[4] The Biorefinery Centre, Institute of Food Research, Norwich Research Park, Colney, Norwich NR4 7UA, UK; E-Mails: david.wilson@ifr.ac.uk (D.R.W.); keith.waldron@ifr.ac.uk (K.W.W.)

* Authors to whom correspondence should be addressed; E-Mails: a.f.lee@aston.ac.uk (A.F.L.); k.wilson@aston.ac.uk (K.W.); Tel.: +44-121-204-4036 (A.F.L. & K.W.).

External Editor: Keith Hohn

Received: 7 October 2014; in revised form: 20 November 2014 / Accepted: 27 November 2014 / Published: 15 December 2014

Abstract: A family of tungstated zirconia solid acid catalysts were synthesised via wet impregnation and subsequent thermochemical processing for the transformation of glucose to 5-hydroxymethylfurfural (HMF). Acid strength increased with tungsten loading and calcination temperature, associated with stabilisation of tetragonal zirconia. High tungsten dispersions of between 2 and 7 W atoms·nm^{-2} were obtained in all cases, equating to sub-monolayer coverages. Glucose isomerisation and subsequent dehydration via fructose to HMF increased with W loading and calcination temperature up to 600 °C, indicating that glucose conversion to fructose was favoured over weak Lewis acid and/or base sites associated with the zirconia support, while fructose dehydration and HMF formation was favoured over Brönsted acidic WO_x clusters. Aqueous phase reforming of steam exploded rice straw hydrolysate and condensate was explored heterogeneously for the first time over

a 10 wt% WZ catalyst, resulting in excellent HMF yields as high as 15% under mild reaction conditions.

Keywords: biomass; solid acid; zirconia; glucose; HMF; tungstate

1. Introduction

The energy and atom efficient transformation of biomass waste feedstocks such as rice, corn and coconut husks, rice and wheat straw, corn cobs and palm kernels into sustainable gasoline and/or diesel drop-in biofuels, offers new routes to environmentally-benign renewable energy resources [1,2]. Furthermore, the attendant production of highly functionalised molecular intermediates affords synthetic pathways to diverse platform bio-derived chemicals which underpin the formulation of plastics and polymers with novel properties [3].

Lignocellulosic biomass comprises cellulose and hemicellulose carbohydrate polymers and lignin poly phenolics, and is susceptible to thermochemical decomposition into their constituent monomers. The cellulosic components are most readily activated and depolymerised into C_5 and C_6 monosaccharides, principally xylose and glucose, respectively, important building blocks for deoxygenation to chemical intermediates such as 5-hydroxymethylfurfural (HMF), levulinic acid and γ-valerolactone , and whose further deoxygenation yields fungible alkane, alkene and aromatic liquid fuels. The primary barrier to HMF utilisation in high-volume chemical and fuel applications is its high cost and correspondingly limited availability. To be commercially viable, large scale HMF production must be achievable at a comparable cost to that of petroleum-derived feedstocks such as para-xylene and terephthalic acid. Glucose or fructose derived from the cellulose component of biomass can be converted into HMF through its stepwise dehydration under mild aqueous conditions. A number of economically viable routes exist to these sugars [4–9], hence HMF production from such bio-derived feedstocks appears an attractive process in terms of the raw material supply and green credentials. Glucose conversion to HMF requires catalysts able to affect its isomerisation to fructose [10], and subsequent dehydration of this fructose intermediate, and poor HMF yields are consequently commonly reported in the literature.

Homogeneous mineral acid catalysed routes to HMF are well-known, however, heterogeneous (solid) variants offer numerous process advantages in terms of product separation, catalyst recycling, acid storage and handling, and opportunities for continuous flow operation. A number of solid acid catalysts have shown potential for this transformation [11–13], with a recent systematic investigation of sulfated zirconia highlighting a bifunctional pathway involving Lewis acid catalysed glucose isomerisation to fructose over the parent zirconia support, and subsequent Brönsted acid catalysed dehydration to HMF, conferring a yield of 2%–3% at 100 °C [14]. Other metal oxides, notably tungstates also exhibit solid acidity, particularly in conjunction with zirconia [11], but have never been applied to aqueous phase HMF production from rice straw.

Herein, we demonstrate the utility of tungstated zirconia for the aqueous phase transformation of hydrolysate sugar (obtained from rice straw lignocellulose hydrolysis) to HMF as a function of tungsten oxide loading and calcination temperature, achieving HMF yields as high as 10%–15% from steam exploded hydrosylate and liquid condensate.

2. Results and Discussion

2.1. Catalyst Characterization

The physicochemical properties of zirconia and WZs are summarised in Table 1 as a function of their calcination temperature and nominal W loading. There is good agreement between the nominal and surface W loadings observed by XPS, with the generally higher observed surface loadings consistent with the wet impregnation protocol employed and consequent concentration of tungsten at the catalyst surface relative to bulk. In almost all cases, tungsten addition increased the surface area relative to the corresponding parent ZrO_2, this effect being most significant at the lower calcination temperature of 500 °C, while the surface areas of all WZ materials decreased with increasing calcination temperature. There was no significant variation in either total pore volume or mean pore diameter, reflecting the non-porous nature of both parent zirconia and WZ, with measured porosity associated with interparticle voids and hence, was relatively insensitive to changes in particle morphology or crystallinity. Acid strength, as measured by the pH of an aqueous suspension of WZ, increased with W loading and calcination temperature (parent ZrO_2), reaching 3.31 for the 10 wt% WZ calcined at 500 °C. It is important to note that such moderate acidity is known to effect glucose dehydration/fructose isomerisation, but should be insufficient to drive further reaction of any HMF product to levulinic and formic acids observed when employing stronger acids [15,16].

Table 1. Physicochemical properties of ZrO_2 and WZ materials as a function of calcination temperature.

Catalyst	Calcination Temperature/°C	pH [a]	Surface W Loading [b]/wt%	Surface Area [c]/$m^2.g^{-1}$	Mesopore Diameter [d]/Å	Total Pore Volume [d]/$cm^3.g^{-1}$	Surface W Density [e] /atoms.nm^{-2}
ZrO_2		5.0	-	78	25	0.19	-
5 wt% WZ	500	5.6	7.7	122	17	0.18	2.1
10 wt% WZ		5.3	12.6	184	17	0.12	2.7
ZrO_2		-	-	44	50	0.15	-
5 wt% WZ	600	5.7	9.3	81	22	0.15	3.7
10 wt% WZ		4.6	8.4	116	17	0.16	3.0
ZrO_2		-	-	86	17	0.19	-
5 wt% WZ	700	5.5	11.7	64	25	0.14	6.0
10 wt% WZ		3.3	17.7	98	20	0.18	7.1

[a] Solution pH; [b] determined by XPS; [c] BET value from porosimetry; [d] Mesopore diameter and total pore volume from porosimetry; [e] Surface W density = W surface loading/[(100 × RMM_W × 6.023 × 10^{23}) × (BET surface area × 10^{18})], RMM_W is the Relative Molecular Weight of tungsten.

The nature of crystalline phases was also investigated via powder X-ray diffraction as a function of W loading and calcination temperature (Figure 1). Tetragonal zirconia (*t*-ZrO_2) is known to be thermodynamically unstable with respect to monoclinic zirconia (*m*-ZrO_2), and indeed the latter phase dominates the diffractograms of the parent support. The intensity of *m*-ZrO_2 reflections also increases with calcination temperature, accompanied by peak sharpening, indicative of an increase in crystallite size. Peak width analysis employing the Scherrer equation confirms the mean crystallite size rises from 10.2 nm after 500 °C calcination to 22 nm following 700 °C treatment, consistent with the decrease in

surface area. In contrast, tungstated zirconias exhibited significant contributions from the *t*-ZrO_2 phase, with the proportion *t*-ZrO_2:*m*-ZrO_2 ratio proportional to the tungsten loading. For the 10 wt% WZ sample, only *t*-ZrO_2 was detectable even after calcination at 700 °C. Tungsten thus serves to stabilise the tetragonal phase with respect to the monoclinic, in accordance with previous reports for sulfated and tungstated zirconia [15,17,18]. Crystallite size for the *t*-ZrO_2 phase in the WZ materials were also far smaller than those of the parent *m*-ZrO_2, varying from 6.6 nm (500 °C) to 9.6 nm (700 °C). No reflections attributable to any tungsten oxide phase were observed for any WZ samples, indicating that tungsten must be highly dispersed, either as sub-2 nm particles or as a monolayer coating over the underlying *t*-ZrO_2 support. The latter hypothesis is in line with the surface W density, which increases with tungsten loading from 2.1 to 7.1 W atoms.nm^{-2}, but in all cases remains below that required to saturate a WO_3 monolayer (8.9 W atoms.nm^{-2}) [19].

Figure 1. Powder XRD patterns for (**A**) parent zirconia, (**B**) 5 wt% WZ, and (**C**) 10 wt% WZ as a function of W loading and calcination temperature showing the thermal stabilisation of *t*-ZrO_2 by surface tungstate.

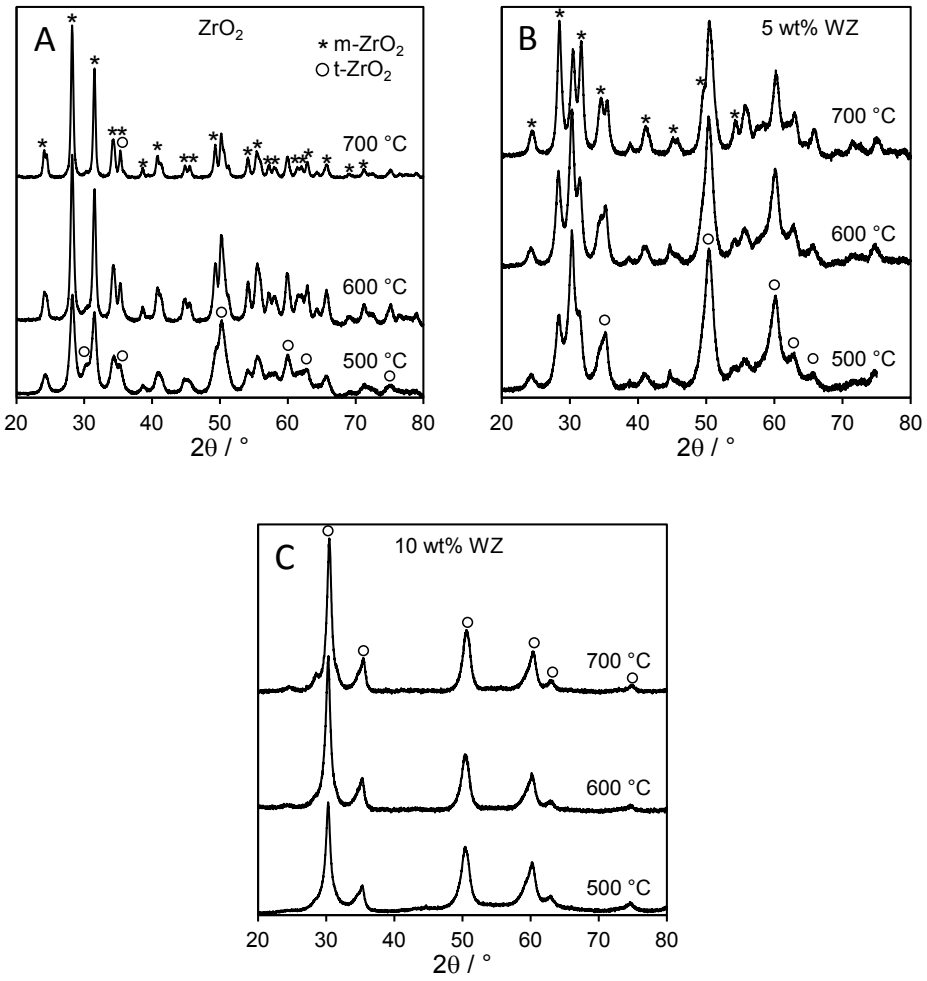

The nature of the surface acid sites was probed through pyridine chemisorption and subsequent DRIFTS analysis to identify the presence of Brönsted and Lewis acid sites and the relative Brönsted:Lewis character. Figure 2 shows the resulting DRIFT vibrational spectra for the parent and WO_x/ZrO_2 solids calcined at 500, 600 and 700 °C, revealing bands at 1540, 1490 and 1440 cm^{-1} typical

of chemisorbed pyridine [19,20]. The band at 1540 cm^{-1} is attributed to a pyridinium ion bound to Brönsted acid sites, while those at 1580 cm^{-1} and 1438 cm^{-1} are attributed to molecular pyridine coordinated to Lewis acid sites. Since the 1488 cm^{-1} band is observed from pyridine adsorbed at both Brönsted and Lewis acid sites, the relative Brönsted:Lewis acidity can be quantified from the ratio of the 1540 cm^{-1} and 1438 cm^{-1} bands, as shown in Figure 2 as a function of calcination temperature and W loading. The Brönsted:Lewis ratio increased significantly with tungsten content, as anticipated upon impregnation of the parent zirconia support, which possesses oxygen deficient Lewis acid centres, with tungstate clusters. Calcination also increased the Brönsted character of all materials, possibly reflecting the formation of two-dimensional polytungstate clusters and attendant charge neutralisation by adsorbed protons [21].

Figure 2. (**left**) DRIFT spectra of chemisorbed pyridine over zirconia and tungstated zirconias; and (**right**) ratio of Brönsted:Lewis adsorption bands as a function of W loading and calcination temperature.

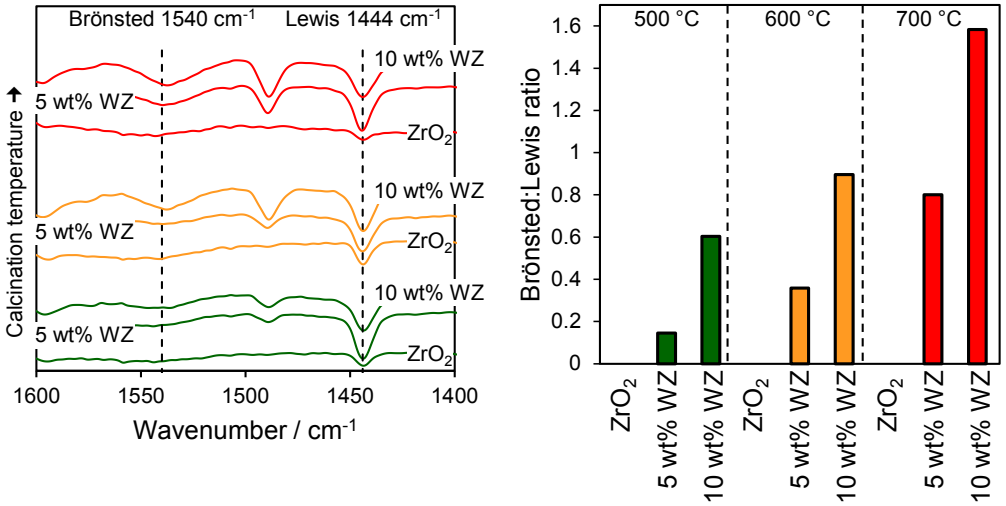

2.2. Catalytic Conversion of Glucose

The impact of tungsten upon glucose isomerisation to fructose and subsequent dehydration to HMF was explored as a function of calcination temperature. In all cases, glucose conversion ranged between 5% and 20% under the mild conditions employed in this work, with Figure 3 revealing a decrease with increasing W loading and calcination temperature. These observations are consistent with another report on WZs, wherein glucose conversion is favoured over weak Lewis acid base sites associated with the bare zirconia support [14], while higher W loadings and calcination temperatures favour Brönsted acid sites which drive fatty acid esterification [19]. We can therefore infer a switchover in Lewis to Brönsted acid character resulting from the coalescence of isolated WO_x clusters as polytungstates and the resultant genesis of Brönsted acidity for the 5 and 10 wt% WZ samples. This observation is in excellent agreement with the pyridine titrations shown in Figure 2. The fall in conversion with temperature also likely reflects the corresponding decreases in surface area due to crystallite sintering. Normalising the final glucose conversion to the acid site density derived from the integrated chemisorbed pyridine DRIFTS intensity, yielded Turnover Frequencies of 4.7, 0.9 and 0.8 h^{-1} for the 700 °C calcined ZrO_2, 5 wt% and 10 wt%

WZ materials, respectively. The superior activity of the parent zirconia is in accordance with its pure Lewis acid character.

Figure 3. Glucose conversion after 6 h reaction at 100 °C over zirconia and tungstated zirconias.

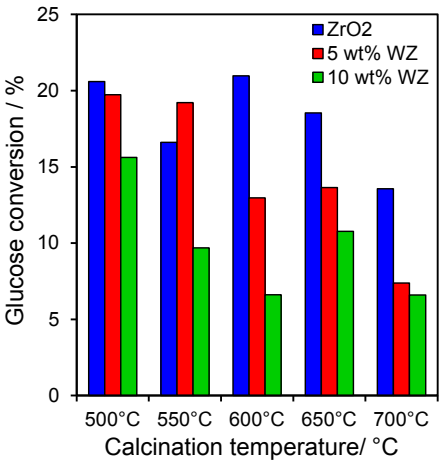

Only two major reaction products were observed from glucose conversion over all WZ materials, fructose via glucose isomerisation, and HMF via dehydration of the reactively-formed fructose. This reflects the low reaction temperatures employed in this study relative to the literature [12] which disfavour HMF polymerisation and humin formation observed in other reports [22]. In all cases, fructose was overwhelmingly the dominant product. However, tungsten incorporation significantly enhanced HMF production, with the 10 wt% WZ sample twice as selective towards the furan as the parent zirconia support (Figure 4). High temperature calcination of WZ suppressed HMF formation at the expense of fructose, clearly indicating two competing reaction pathways, each requiring different active sites. Fructose appears favoured by Lewis acid sites present over the parent zirconia, whereas HMF is favoured by moderate surface tungstate densities of 2–3 atoms.nm^{-2}, significantly less than required to form a full monolayer (which impart Brönsted acidity), and calcination around 600 °C wherein surface areas remained around 100 m^2 g^{-1}. Fructose dehydration to HMF hence appears catalysed by isolated or dimeric WO_x clusters.

Figure 4. (**left**) Selectivity to fructose; and (**right**) HMF production from glucose after 6 h reaction at 100 °C over zirconia and tungstated zirconias.

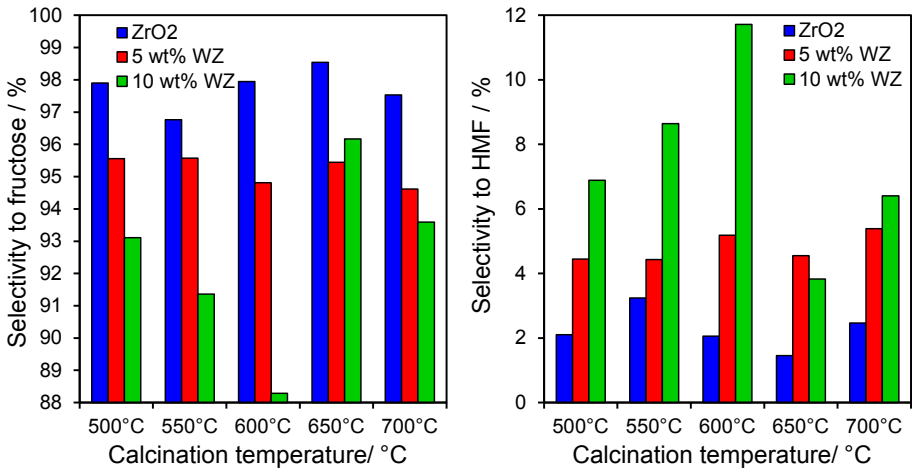

2.3. Catalytic Conversion of Fructose

In order to confirm the preceding hypothesis, namely that glucose isomerisation occurs over Lewis acid sites whereas fructose dehydration is favoured by Brönsted acid sites associated with small tungstate clusters, the behaviour of our WZ series was also assayed for the direct dehydration of fructose (Figure 5). Activities were slightly higher than those observed for glucose, with fructose conversions spanning approximately 10%–30%. However, in contrast, regarding their reactivity to glucose, the WZ catalysts always outperformed the parent zirconia, consistent with their predominant Brönsted acidity observed by pyridine titration, and conferred significant conversion even at high calcination temperatures, despite the large decrease in BET surface areas; in contrast, calcination deactivated the pure zirconia. These observations are fully consistent with the notion that fructose dehydration occurs faster over WO_x Brönsted acid sites than Lewis acid sites on the parent ZrO_2 support.

Figure 5. Fructose conversion after 6 h reaction at 100 °C over zirconia and tungstated zirconias.

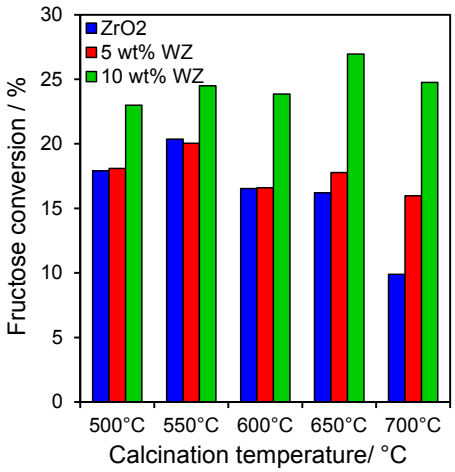

Figure 6. Selectivity to HMF production from fructose after 6 h reaction at 100 °C over zirconia and tungstated zirconias.

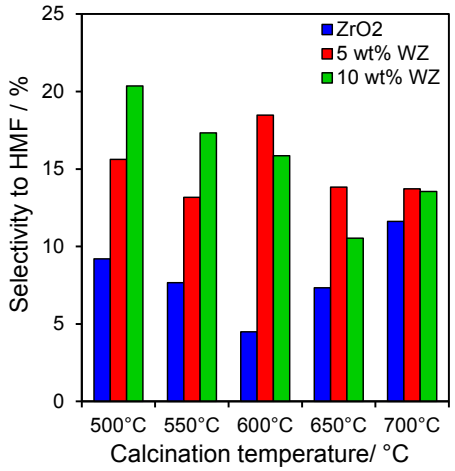

HMF (and trace oligomers of its condensation products), alongside glucose formed via the reversible isomerisation reaction, were the major products of fructose dehydration, with the WZ samples significantly more selective to HMF than ZrO_2 (Figure 6), with the highest selectivities of 15%–20%

observed after moderate thermal processing of the 5 wt% and 10 wt% WZ catalysts, equating to a three-fold higher HMF yield, a consequence of the superior Brönsted acid character of the tugstated materials which favour rapid fructose dehydration over isomerisation back to glucose.

2.4. Catalytic Dehydration of Hydrolysate Sugar and Condensate

Having demonstrated the efficacy of WZ towards conversion of glucose and fructose model reactants, the behaviour of the 500 °C calcined materials was explored towards the transformation of hydrolysate sugar and condensate derived from Vietnamese rice straw. These catalysts were selected since they exhibited the optimum balance of glucose/fructose conversion and selectivity to HMF. The results in Figure 7 show similar poor levels of glucose conversion within both the hydrolysate and condensate at 100 °C for all three catalysts, with the parent zirconia the most active in accordance with Figure 3 and it superior Lewis acidity (Figure 2) which is required to drive initial glucose isomerisation to fructose. However, even a small increase in reaction temperature to 130 °C dramatically enhanced catalyst activity, with conversion climbing to around 30%–40% for the hydrosylate and 50%–60% for the condensate. At these higher reaction temperatures, the 10 wt% WZ also now outperformed zirconia towards both feedstocks.

Figure 7. Glucose conversion after 6 h reaction at 100 °C from (**left**) hydrolysate; and (**right**) condensate over zirconia and tungstated zirconias.

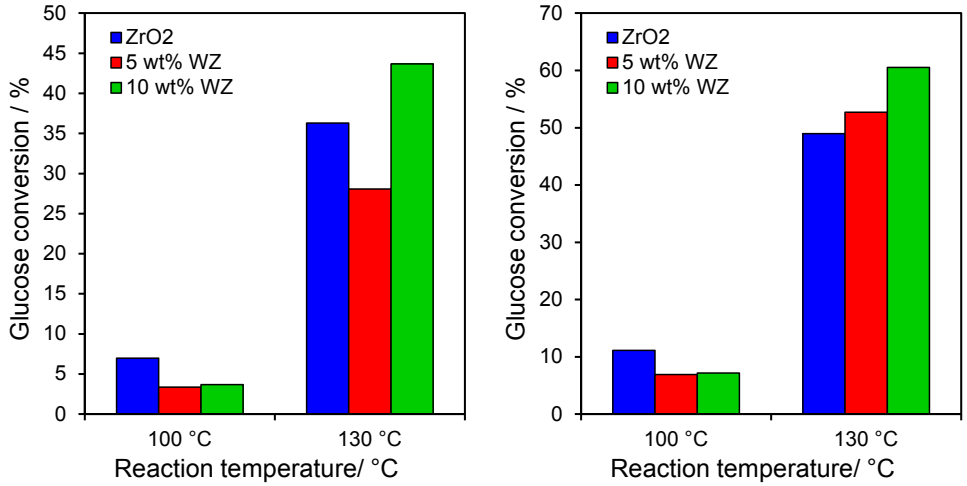

The slight rise in reaction temperature enhanced overall product yields from ~10% to between 25%–35% from both hydrolysate and condensate. Fructose was the primary product in almost all circumstances, with the observed acetic acid reflecting that present in the starting feedstocks and remaining essentially unchanged during reaction (equating to ~3.5 $g \cdot L^{-1}$ in the hydrolysate and 2.5 $g \cdot L^{-1}$ in the condensate). HMF and furfural production (the latter presumably formed from trace hemicellulose via dehydration of xylose) increased dramatically at 130 °C, seen in Figure 8, particularly in the condensate wherein HMF actually becomes the principal product over the 10 wt% WZ catalyst with a yield of ~15%. This is a noteworthy achievement since it is difficult to obtain high HMF yields under aqueous reaction conditions due to competing HMF hydrolysis and resultant levulinic and formic acid formation, coupled with further degradation and polymerisation reactions to humins.

Figure 8. Yield of major products after 6 h reaction of processed rice straw at 100 °C and 130 °C.

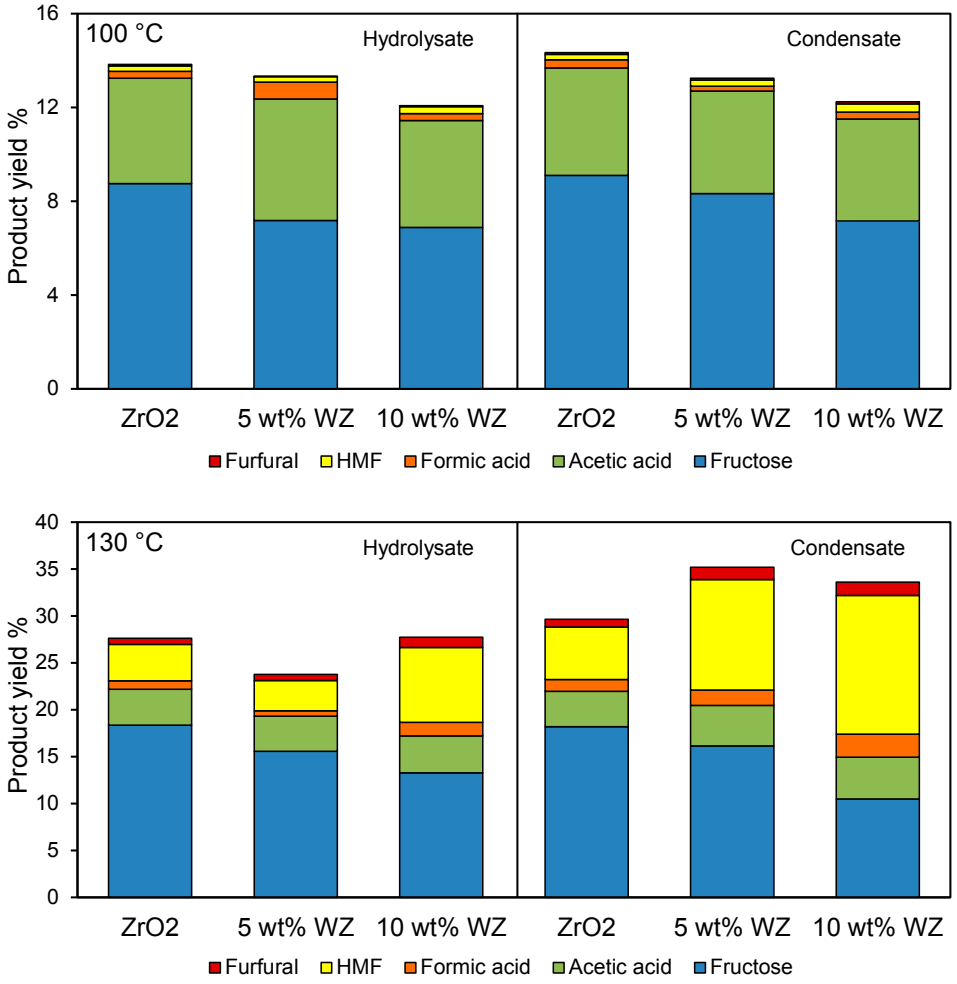

3. Experimental Section

3.1. Catalyst Preparation

WO_3/ZrO_2 (WZ) catalysts were prepared with 5 and 10 wt% W loadings via wet impregnation of zirconium hydroxide (MelChem XZO 880/01, MEL Chemicals Company, Manchester, UK) with 40 cm^3 aqueous ammonium (para)tungstate hydrate solution (Sigma-Aldrich, Manchester, UK). The resulting slurry was stirred for 15 h at room temperature, and subsequently dried to evaporation overnight at 80 °C prior to calcination under flowing oxygen (10 $cm^3 \cdot min^{-1}$) between 500 and 700 °C for 4 h. Pure zirconia controls were prepared by direct calcination of the parent zirconium hydroxide at different temperatures.

3.2. Catalyst Characterization

Textural properties of the WZ materials were characterised by nitrogen porosimetry using a Quantachrome Nova 1200 (Quantachrome, Oxford, UK) porosimeter and analysed with NovaWin software version 11. (Quantachrome, Oxford, UK) Samples were degassed at 120 °C for 2 h prior to analysis of adsorption/desorption isotherms by nitrogen physisorption at −196 °C. BET surface areas were calculated over the relative pressure range 0.01–0.2.

XPS was performed on a Kratos Axis HSi X-ray photoelectron spectrometer fitted (Kratos Analytical, Manchester, UK) with a charge neutraliser and magnetic focusing lens, employing Al K_α monochromated radiation (1486.7 eV). Spectral fitting was performed using CasaXPS version 2.3.14. (Casa Software Ltd., Teignmouth, UK) High-resolution O 1s, S 2p, Zr 3d and W 4f spectral binding energies were corrected to the C 1s peak at 284.6 eV and surface atomic compositions calculated via correction for the appropriate instrument response factors. pH measurements on aqueous catalyst suspensions were performed by adding 0.1 g of each catalyst to 20 mL of deionised water and stirring at room temperature for 30 min. Solution pH was subsequently measured using a Jenway 3305 pH meter (Jenway, Dunmow, UK). Powder X-ray diffraction patterns were recorded on a (PANalytical, Almelo, Holland) X'pert-Pro diffractometer (PANalytical, Almelo, Holland) fitted with an X'celerator detector (PANalytical, Almelo, Holland) with a Cu K_α (1.54 Å) source and nickel filter, and calibrated against a quartz standard. Brönsted/Lewis acid character was determined via Diffuse Reflectance Infrared Fourier Transform Spectroscopy (DRIFTS) on a Nicolet Nexus 479 FTIR spectrometer (Nicolet, MN, USA) via pyridine adsorption; approximately 1 mL of pyridine (99.8%, Sigma-Aldrich, UK) was dropped onto 200 mg of sample and dried by vacuum oven to remove physisorbed base.

3.3. Catalytic Reaction

Control experiments employing glucose and fructose as substrates were conducted employing 0.55 mmol dissolved in the 20 mL deionized water and 100 mg catalyst. Reactions were undertaken using a Radleys Starfish system within glass round-bottomed flasks at 100 °C for 6 h under stirring at 300 rpm. The reaction mixture was periodically sampled, with aliquots analysed with an Agilent 1200 series HPLC (Agilent, Oxford, UK) equipped with refractive index and UV diode array detectors and a Hi-Plex H column (Agilent, Oxford, UK) maintained at 65 °C under a 5 mM H_2SO_4 mobile phase flowed at 0.6 cm^3 min^{-1}.

Field grown rice (*Oryza sativa*, *cv.* KhangDan18) straw and husk was harvested at maturity in spring 2012 at the Ba Vi National Park, Hanoi, Vietnam. Both rice straw and husk were steam exploded into hot water using a bespoke CAMBI™ steam explosion facility with a 30 L reactor (Cambi AS, Asker, Norway). Before steam explosion, the rice straw was cut into 2–3 cm pieces for reactor loading. The reactor was charged with 500 g feedstock, sealed and heated (husk: 220 °C; straw: 210 °C) with steam for 10 min. After this time, the contents were released (steam explosion), and deposited into 3.5 L hot water via a collection cyclone. The reactor was then pressurised again to 2–3 bar and released to dislodge any residue. The resulting pretreated slurry was collected and fractionated into solid and liquid phases by centrifuging through a 100 μm nylon mesh. The insoluble residue was rinsed extensively to ensure that any water-soluble material was removed. The residue was quantified and stored at −40 °C prior to further use or analysis.

Pilot-scale hydrolyses (5 L) were conducted in a bespoke high-torque bioreactor [23]. Digests were conducted at 20 *w*/*v*% substrate concentration using 1 Kg dry weight equivalent of steam exploded rice straw/husk suspended in sodium acetate/acetic acid buffer (4.1 g/L, pH 5.0). The buffer and substrate were initially heated to >85 °C to minimise the possibility of microbial contamination. The mixture was then cooled to 50 °C and an appropriate quantity of Cellic®CTec2 (Novozymes, Bagsværd, Denmark) was added (6.49 or 10 filter paper unit/g dry matter for straw and husk, respectively). The hydrolysate

was agitated at 39 rpm for 4 days and the resulting aqueous solution contained 8.7 wt% glucose, while the steam exploded liquid condensate fraction contained 2.7 wt% glucose. Reactions were carried out as described above at 100 °C and 130 °C. Glucose and fructose conversion, product selectivity and yields are quoted ±2%, with mass balances >95%.

4. Conclusions

Here, we report the first application of a solid acid catalyst for the production of HMF from hydrolysate and condensate streams produced via the steam explosion of rice straw. Tungstated zirconia catalysts having 5 and 10 wt% W were prepared via wet impregnation and calcined at 500–700 °C to investigate the optimum WO_x surface density and Lewis:Brönsted ratio for the direct conversion of glucose to HMF under the mild conditions. In all cases, glucose conversion over WZ catalysts ranged between 5% and 20%, with HMF selectivity increasing with W loading and calcination temperature up to 600 °C. In comparison, reaction of pure fructose resulted in higher conversions of 10%–30%, for WZ, which always outperformed the parent zirconia, while being relatively insensitive to high calcination temperatures. These combined observations are consistent with the notion that glucose conversion to fructose is favoured over weak Lewis acid and/or base sites observed for the bare zirconia support, while fructose dehydration and HMF formation occurs preferentially over WO_x Brönsted acid sites, the latter being favoured for high W loadings and calcination temperatures. Application of the optimum 500 °C calcined 10 wt% WZ catalyst in the aqueous phase conversion of rice straw hydrolysate and condensate at 130 °C revealed fructose, HMF and furfural were the main products formed (the latter presumably formed from trace hemicellulose via dehydration of xylose). When using condensate from steam exploded rice straw, HMF actually becomes the principal product with a yield of ~15%, which is a noteworthy achievement under aqueous reaction since this is obtained on a crude feedstock containing impurities such as acetic acid, xylose and formic acid.

Acknowledgments

We thank the EPSRC for funding under (EP/K000616/1 and EP/G007594/4) and MEL Chemicals for the supply of $Zr(OH)_4$, and BBSRC for funding (BB/J013838/1 and Institute Strategic Programme "Food and Health" BB/J004545/1). KW acknowledges The Royal Society for the award of an Industry Fellowship, and AFL thanks the EPSRC for the award of a Leadership Fellowship. The authors acknowledge financial support from CAPES (Coordenação de Aperfeiçoamento de Pessoal de Nível Superior), CNPq (Conselho Nacional de Desenvolvimento Cientifico e Tecnológico) and UFPR (Universidade Federal do Paraná). We also acknowledge Peter Ryden for assistance with rice straw/husk digestion.

Author Contributions

K.W. and A.F.L. conceived the research programme and drafted the manuscript; G.C., A.M. and V.C.S. synthesised, characterised and tested the catalysts; D.R.W. and K.W.W. supervised the steam explosion and digestion experiments.

Conflicts of Interest

The authors declare no conflict of interest.

References

1. Lee, A.F.; Bennett, J.A.; Manayil, J.C.; Wilson, K. Heterogeneous catalysis for sustainable biodiesel production via esterification and transesterification. *Chem. Soc. Rev.* **2014**, *43*, 7887–7916
2. Wilson, K.; Lee, A.F. Rational design of heterogeneous catalysts for biodiesel synthesis. *Catal. Tech. Sci.* **2012**, *2*, 884–897.
3. Lee, A. Catalysing sustainable fuel and chemical synthesis. *Appl. Petrochem. Res.* **2014**, *4*, 11–31.
4. Pilipski, M. Saccharification of cellulose. U.S. Patent 4,235,968, 25 November 1980.
5. Onda, A.; Ochi, T.; Yanagisawa, K. Selective hydrolysis of cellulose into glucose over solid acid catalysts. *Green Chem.* **2008**, *10*, 1033–1037.
6. Pang, J.; Wang, A.; Zheng, M.; Zhang, T. Hydrolysis of cellulose into glucose over carbons sulfonated at elevated temperatures. *Chem. Commun.* **2010**, *46*, 6935–6937.
7. Zhou, C.H.; Xia, X.; Lin, C.X.; Tong, D.S.; Beltramini, J. Catalytic conversion of lignocellulosic biomass to fine chemicals and fuels. *Chem. Soc. Rev.* **2011**, *40*, 5588–5617.
8. Climent, M.J.; Corma, A.; Iborra, S. Converting carbohydrates to bulk chemicals and fine chemicals over heterogeneous catalysts. *Green Chem.* **2011**, *13*, 520–540.
9. Kobayashi, H.; Fukuoka, A. Synthesis and utilisation of sugar compounds derived from lignocellulosic biomass. *Green Chem.* **2013**, *15*, 1740–1763.
10. Moliner, M.; Román-Leshkov, Y.; Davis, M.E. Tin-containing zeolites are highly active catalysts for the isomerization of glucose in water. *Proc. Natl. Acad. Sci. USA* **2010**, *107*, 6164–6168.
11. Chareonlimkun, A.; Champreda, V.; Shotipruk, A.; Laosiripojana, N. Reactions of C_5 and C_6-sugars, cellulose, and lignocellulose under hot compressed water (HCW) in the presence of heterogeneous acid catalysts. *Fuel* **2010**, *89*, 2873–2880.
12. Nakajima, K.; Baba, Y.; Noma, R.; Kitano, M.; N. Kondo, J.; Hayashi, S.; Hara, M. $Nb_2O_5 \cdot nH_2O$ as a heterogeneous catalyst with water-tolerant lewis acid sites. *J. Am. Chem. Soc.* **2011**, *133*, 4224–4227.
13. Zeng, W.; Cheng, D.G.; Chen, F.; Zhan, X. Catalytic conversion of glucose on Al–Zr mixed oxides in hot compressed water. *Catal. Lett.* **2009**, *133*, 221–226.
14. Osatiashtiani, A.; Lee, A.F.; Brown, D.R.; Melero, J.A.; Morales, G.; Wilson, K. Bifunctional SO_4/ZrO_2 catalysts for 5-hydroxymethylfufural (5-HMF) production from glucose. *Catal. Tech. Sci.* **2014**, *4*, 333–342.
15. Qi, X.; Watanabe, M.; Aida, T.M.; Smith, R.L., Jr. Sulfated zirconia as a solid acid catalyst for the dehydration of fructose to 5-hydroxymethylfurfural. *Catal. Comm.* **2009**, *10*, 1771–1775.
16. Climent, M.J.; Corma, A.; Iborra, S. Conversion of biomass platform molecules into fuel additives and liquid hydrocarbon fuels. *Green Chem.* **2014**, *16*, 516–547.
17. Chen, F.R.; Coudurier, G.; Joly, J.F.; Vedrine, J.C. Superacid and catalytic properties of sulfated zirconia. *J. Catal.* **1993**, *143*, 616–626.
18. López, D.E.; Suwannakarn, K.; Bruce, D.A.; Goodwin Jr., J.G. Esterification and transesterification on tungstated zirconia: Effect of calcination temperature. *J. Catal.* **2007**, *247*, 43–50.

19. Dos Santos, V.C.; Wilson, K.; Lee, A.F.; Nakagaki, S. Physicochemical properties of WO_x/ZrO_2 catalysts for palmitic acid esterification. *Appl. Catal. B* **2015**, *162*, 75–84.
20. Karim, A.H.; Triwahyono, S.; Jalil, A.A.; Hattori, H. WO_3 monolayer loaded on ZrO_2: Property-activity relationship in *n*-butane isomerization evidenced by hydrogen adsorption and IR studies. *Appl. Catal. A* **2012**, *433–434*, 49–57.
21. Barton, D.G.; Shtein, M.; Wilson, R.D.; Soled, S.L.; Iglesia, E. Structure and electronic properties of solid acids based on tungsten oxide nanostructures. *J. Phys. Chem. B* **1999**, *103*, 630–640.
22. Hu, X.; Lievens, C.; Larcher, A.; Li, C.Z. Reaction pathways of glucose during esterification: Effects of reaction parameters on the formation of humin type polymers. *Bioresour. Technol.* **2011**, *102*, 10104–10113.
23. Elliston, A.; Collins, S.R.A.; Wilson, D.R.; Roberts, I.N.; Waldron, K.W. High concentrations of cellulosic ethanol achieved by fed batch semi simultaneous saccharification and fermentation of waste-paper. *Bioresour. Technol.* **2013**, *134*, 117–126.